

JET-P(92)12

J.A. Wesson, T.C. Render
and JET Team

Theory of Marfe Stability

“This document contains JET information in a form not yet suitable for publication. The report has been prepared primarily for discussion and information within the JET Project and the Associations. It must not be quoted in publications or in Abstract Journals. External distribution requires approval from the Publications Officer, JET Joint Undertaking, Abingdon, Oxon, OX14 3EA, UK”.

“Enquiries about Copyright and reproduction should be addressed to the Publications Officer, EFDA, Culham Science Centre, Abingdon, Oxon, OX14 3DB, UK.”

The contents of this preprint and all other JET EFDA Preprints and Conference Papers are available to view online free at www.iop.org/Jet. This site has full search facilities and e-mail alert options. The diagrams contained within the PDFs on this site are hyperlinked from the year 1996 onwards.

Theory of Marfe Stability

J.A. Wesson, T.C. Render
and JET Team*

JET-Joint Undertaking, Culham Science Centre, OX14 3DB, Abingdon, UK

¹*UKAEA/ Euratom Fusion Association, Culham Laboratory, Abingdon, Oxon*
** See Annex*

Preprint of Paper to be submitted for publication in
Nuclear Fusion

Theory of Marfe Stability

J.A. Wesson and T.C. Hender *

JET Joint Undertaking, Abingdon, Oxfordshire, United Kingdom

*UKAEA/Euratom Fusion Association, Culham Laboratory,
Abingdon, Oxfordshire, United Kingdom

The theory of marfe stability is generalised by using the equilibrium temperature as the independent variable. The description incorporates both perpendicular and parallel transport.

1. INTRODUCTION

The name marfe is given to the toroidally symmetric, but poloidally asymmetric, band of impurity radiation observed in tokamaks. This phenomenon is the result of an instability which arises when a local change in the radiated power, brought about by a temperature perturbation, is greater than the compensatory heat flow induced by the temperature change. [1, 2, 3]

The instability takes place in the outer region of the plasma where the temperature is low and the impurity radiation is correspondingly high. Stability depends not only on the temperature but also on the temperature profile in the region where it is formed. The straightforward way of solving the problem is first to obtain an equilibrium solution for the temperature in the presence of the radiation for each particular case, and then to calculate its stability. We shall here use a method which combines these processes and leads to a general but simple stability diagram.

2. THEORY

2.1 Basic Equation

The analysis is based on the heat balance equation

$$\nabla \cdot K \nabla T = n n_i R(T) \quad (1)$$

where, since the marfe instability occurs in a narrow layer near the edge of the plasma, heat sources are neglected. The thermal conductivity has a value K_{\parallel} parallel to the magnetic field and a value K_{\perp} perpendicular to the field, n and n_i are the electron and impurity densities and $R(T)$ is the radiation function. The radiation function is peaked, becoming small at both low and high temperatures.

2.2 Equilibrium

The equilibrium is taken to be a function only of the minor radial coordinate r and since we are only concerned with a region near the edge of the plasma we can write

$$K_{\perp} \frac{d^2 T}{dr^2} = nn_i R(T) \quad (2)$$

It will be assumed that the radial variation of the equilibrium values of n , and K_{\perp} is sufficiently small that they can be regarded as constants.

We shall shortly need an expression for the equilibrium temperature gradient. This can be obtained by multiplying equation (2) by dT/dr and integrating with respect to r to obtain

$$K_{\perp} \left(\frac{dT}{dr} \right)^2 = K_{\perp} \left(\frac{dT}{dr} \right)_+^2 - 2nn_i \int_T^{\infty} R(T) dT \quad (3)$$

where $(dT/dr)_+$ is the temperature gradient on the high temperature side of the radiation layer where the radiation has become negligible, and the limit in the integral is correspondingly taken to be $T \rightarrow \infty$.

2.3 Perturbation Equation

The linearised form of equation (1) is

$$K_{\perp} \frac{d^2 \tilde{T}}{dr^2} - K_{\parallel}(T) k_{\parallel}^2 \tilde{T} = nn_i \left\{ \left(\frac{\tilde{n}}{n} + \frac{\tilde{n}_i}{n_i} \right) R(T) + R'(T) \tilde{T} \right\} \quad (4)$$

The parallel thermal conductivity K_{\parallel} is proportional to $T^{5/2}$. For the most unstable mode \tilde{T} varies as $\cos \theta$ and the wave-number $k_{\parallel} = 1/R_0 q$ where R_0 is the major radius of the plasma and q is the safety factor.

We use the equation for pressure balance along the magnetic field to write

$$\frac{\tilde{n}}{n} = - \frac{\tilde{T}}{T}$$

and assume that $n_i \propto n$ so that

$$\frac{\tilde{n}_i}{n_i} = - \frac{\tilde{T}}{T} .$$

Equation (4) then becomes

$$K_{\perp} \frac{d^2 \tilde{T}}{dr^2} - K_{\parallel}(T) k_{\parallel}^2 \tilde{T} = nn_i T^2 \frac{d}{dT} \left(\frac{R(T)}{T^2} \right) \tilde{T} ,$$

or, writing

$$\phi(T) = - T^2 \frac{d}{dT} \left(\frac{R(T)}{T^2} \right) ,$$

$$K_{\perp} \frac{d^2 \tilde{T}}{dr^2} = \left(K_{\parallel}(T) k_{\parallel}^2 - nn_i \phi(T) \right) \tilde{T} . \quad (5)$$

Equation (5) is the marginal stability equation. That is, the thermal equilibria for which the solutions of equation (5) satisfy the appropriate boundary conditions are marginally stable and these equilibria establish the marfe stability boundary.

2.4 Coupling Transformation - Stability Equation

The independent variable in equation (5) is r and the coefficients involve the equilibrium temperature $T(r)$. The stability problem would be simplified if it were possible to change the independent variable to T . This would mean that all equilibria could be covered by solving the resulting equation for \tilde{T} .

The required transformation can be achieved by coupling the equilibrium equations and the stability equation.

Thus using equations (2) and (3) in the relation

$$\frac{d^2 \tilde{T}}{dr^2} = \left(\frac{dT}{dr} \right)^2 \frac{d^2 \tilde{T}}{dT^2} + \frac{d^2 T}{dr^2} \frac{d\tilde{T}}{dT} \quad (6)$$

and substituting into equation (5) gives

$$\left(K_{\perp} \left(\frac{dT}{dr} \right)_+^2 - 2nn_i \int_T^{\infty} R(T) dT \right) \frac{d^2 \tilde{T}}{dT^2} + nn_i R(T) \frac{d\tilde{T}}{dT} = (K_{\parallel}(T)k_{\parallel}^2 - nn_i \phi(T)) \tilde{T} \quad (7)$$

We now define the variables

$$\Lambda_{\perp} = \frac{K_{\perp}}{nn_i} \left(\frac{dT}{dr} \right)_+^2$$

$$\Lambda_{\parallel} = \frac{k_{\parallel}^2}{nn_i} \left(\frac{K_{\parallel}}{T^{5/2}} \right)$$

$$S(T) = \int_T^{\infty} R(T) dT$$

where we note that $K_{\parallel}/T^{5/2}$ is independent of temperature. Although Λ_{\perp} and Λ_{\parallel} are the natural parameters of the problem they are not dimensionless and their dimensions are different. Using these definitions we can now re-write equation (7) in its final form

$$(\Lambda_{\perp} - 2S) \tilde{T}'' = -R\tilde{T}' + (\Lambda_{\parallel} T^{5/2} - \phi) \tilde{T} \quad (8)$$

where S , R and ϕ are all defined functions of T and the primes denote differentiation with respect to T . Equation (8) is the required equation for marginal marfe stability.

2.5 Stability Diagram

Equation (8) has been solved numerically to obtain the relationship between Λ_{\perp} and Λ_{\parallel} at marginal stability. The results obtained for carbon impurity using a coronal model for $R(T)$ [4] are shown in Fig. 1. The coronal model is applied over the temperature range of the principal radiation peak, $3\text{eV} < T < 30\text{eV}$, and is extended below 3eV and above 30eV using an exponential decay. The boundary condition on the higher temperature side is $\tilde{T} \rightarrow 0$. The general boundary condition at $T = 0$ is $\tilde{T} + c \tilde{T}' = 0$. Within the framework of the present theory the appropriate physical boundary condition appears to be that there is no perturbed heat flow across the boundary so that $\tilde{T}'(0) = 0$, and Fig. 1 gives the results for this case. More generally it is possible that the mixed boundary condition is applicable, the value of c depending on the physical conditions. For

calculation for the limiting case $\tilde{T} = 0$ has also been carried out and the results are given in Fig. 2.

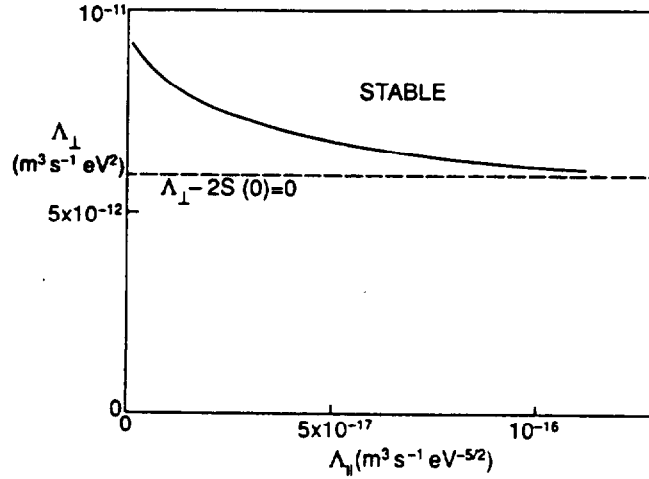


Fig. 1. Stability diagram in the $(\Lambda_{\perp}, \Lambda_{\parallel})$ plane showing the stability boundary for the boundary condition $\tilde{T}'(0) = 0$ together with the radiation contraction stability boundary $\Lambda_{\perp} = 2 S(0)$.

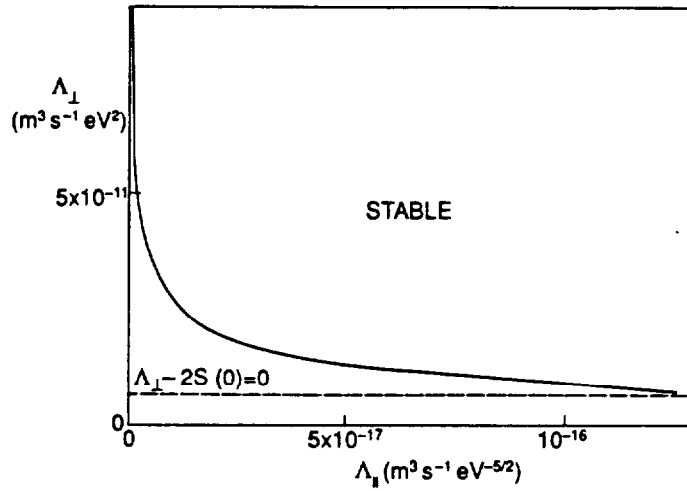


Fig. 2. Stability diagram for the limiting case $\tilde{T}(0) = 0$.

The stability diagram has three regions, the region above the critical Λ_{\perp} being stable to marfes. Below this line marfes become unstable but the unstable region is bounded below at the line $\Lambda = 2 S(0)$. The physical significance of this line is clear from equation (3), which can be written

$$\frac{K_{\perp}}{nn_i} \left(\frac{dT}{dr} \right)^2 = \Lambda_{\perp} - 2S$$

We see that $\Lambda_{\perp} = 2 S(0)$ corresponds to $dT/dr = 0$ at the edge of the plasma and consequently to 100% radiated power. This is the condition for plasma detachment and is therefore an approximate necessary condition for a radiation contraction disruption. Thus, in the appropriate circumstances, a decrease in Λ_{\perp} , caused say by an increase in nn_i , can lead first to a marfe and subsequently to a disruption.

3. ANALYSIS

Some insight into the solutions can be obtained by examining equation (8). This equation presents a standard eigenvalue problem, the solutions giving the required eigen-relationship $\Lambda_{\perp}(\Lambda_{\parallel})$ when the appropriate boundary conditions are satisfied. The achievement of an eigen-solution depends upon the right hand side providing a sufficient negative contribution to \tilde{T}'' . We shall now analyse the behaviour by considering three regimes of Λ_{\parallel} . First we shall consider large Λ_{\parallel} for which the marfe is stable, then we derive an approximate expression for the critical value, $\Lambda_{\parallel c}$, at which instability becomes possible, and finally we calculate the behaviour in the limit $\Lambda_{\parallel} \rightarrow 0$. It should be noted that, for a given magnetic configuration decreasing Λ_{\parallel} means increasing nn_i .

i) Large Λ_{\parallel}

In the limit $\Lambda_{\parallel} \rightarrow \infty$ the positive term involving Λ_{\parallel} dominates. It is reasonable to assume that the radiation function R is zero at very small temperatures and then, despite the $T^{5/2}$ dependence of the parallel conduction term, there will be stability for all Λ_{\perp} as $\Lambda_{\parallel} \rightarrow \infty$.

ii) $\Lambda_{\parallel} = \Lambda_{\parallel c}$

As Λ_{\parallel} is reduced a critical value, $\Lambda_{\parallel c}$, is reached below which instability is possible. The instability first appears at $\Lambda_{\perp} = 2 S(0)$ corresponding to the condition $dT/dr = 0$ at the edge of the plasma and to the smallest possible value of Λ_{\perp} . For $\Lambda_{\parallel} > \Lambda_{\parallel c}$ the plasma is stable to marfes for all Λ_{\perp} .

The essential functional dependence of $\Lambda_{\parallel c}$ can be obtained by writing equation (8) in the approximate form

$$(\Lambda_{\perp} - 2S_m)\tilde{T}'' = \left(\Lambda_{\parallel} T_m^{5/2} - \phi_m - \frac{1}{2} \phi_m'' (T - T_m)^2 \right) \tilde{T} \quad (9)$$

where the subscript m refers to the value at the temperature, for T_m , for which ϕ is a maximum, and ϕ has been expanded about this temperature. Equation (9) can now be written

$$\frac{d^2\bar{T}}{dz^2} + \left(\frac{\phi_m - \Lambda_{\parallel} T_m^{5/2}}{(\Lambda_{\perp} - 2S_m)^{1/2} (-\frac{1}{2}\phi_m'')^{1/2}} - z^2 \right) \bar{T} = 0 \quad (10)$$

where

$$z = \left(\frac{-\frac{1}{2}\phi_m''}{(\Lambda_{\perp} - 2S_m)} \right)^{1/4} (T - T_m) .$$

Equation (10) is Schrödinger's equation for the harmonic oscillator and the lowest eigenvalue is given by

$$\frac{\phi_m - \Lambda_{\parallel} T_m^{5/2}}{(\Lambda_{\perp} - 2S_m)^{1/2} (-\frac{1}{2}\phi_m'')^{1/2}} = 1$$

so that the critical value $\Lambda_{\parallel c}$ at which $\Lambda_{\perp} = 2S(0)$ is given by

$$\Lambda_{\parallel c} = \frac{1}{T_m^{5/2}} \left(\phi_m - (S(0) - S_m)^{1/2} (-\phi_m'')^{1/2} \right) .$$

This result is of course only approximate. It does however show how the range of unstable Λ_{\parallel} increases with increasing amplitude of the radiation term ϕ_m and decreasing T_m . Since ϕ_m'' is negative and $S(0) > S_m$, the final term shows the destabilising effect of a broader ϕ function as characterised by ϕ_m'' .

The onset of instability at $\Lambda_{\perp} = 2S(0)$ can be understood by recalling that, from equation (3), the condition $\Lambda_{\perp} \approx 2S(0)$ corresponds to a small equilibrium temperature gradient. The effect of this is to extend the width of the region over which the radiation terms are significant. This in turn increases the characteristic length involved in the perpendicular thermal conduction, reducing the perpendicular heat flow and allowing instability. The effect is illustrated in Fig. 3. where cases with large and small equilibrium temperature gradients are shown.

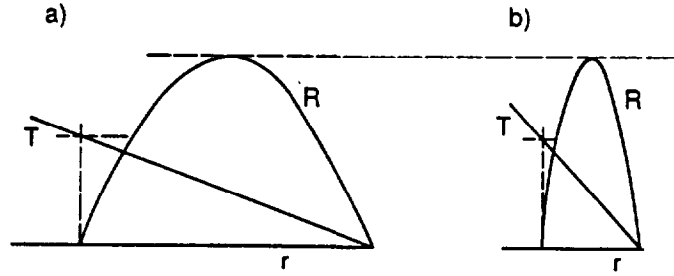


Figure 3 Illustrating the dependence of the radiation layer on the temperature gradient. a) Small equilibrium temperature gradient, for which the radiation function $R(T)$ gives a broad radiation layer. b) Larger equilibrium temperature gradient giving a narrower radiation function and hence greater stabilising perpendicular thermal conduction.

iii) Small Λ_{\parallel}

For the boundary condition $\tilde{T}'(0) = 0$ the nature of the solution at low Λ_{\parallel} is quite different from that for $\tilde{T}(0) = 0$. Whereas in the case $\tilde{T}(0) = 0$ a change of \tilde{T}' of the order of \tilde{T}/T_m is required across the radiation layer, for $\tilde{T}'(0) = 0$ only a very small change in \tilde{T}' is required. The functional behaviour can be derived analytically as follows.

For small Λ_{\parallel} , the solution has a slow decay for temperatures just above those at which R is significant, the right-hand side of equation (8) being proportional to Λ_{\parallel} , and so \tilde{T}'/\tilde{T} is small. Since the boundary condition is $\tilde{T}'(0) = 0$, this means that throughout the whole region where R is significant we have \tilde{T}'/\tilde{T} small. Thus, using $\Lambda_{\perp} \gg 2S$, the equation in the radiation regime is

$$\Lambda_{\perp} \tilde{T}'' = -\phi \tilde{T}$$

and hence

$$\tilde{T}' = -\frac{\tilde{T}}{\Lambda_{\perp}} \int_0^T \phi dT$$

so that the solution just beyond the radiation regime satisfies

$$\frac{\tilde{T}'}{\tilde{T}} = -\frac{c_1}{\Lambda_{\perp}} \tag{11}$$

where c_1 is a constant. At higher temperatures R is small, and equation (8) becomes

$$\tilde{T}'' = \frac{\Lambda_{\parallel}}{\Lambda_{\perp}} T^{5/2} \tilde{T}$$

or

$$\frac{d^2 \tilde{T}}{dx^2} = x^{5/2} \tilde{T} \quad (12)$$

where

$$x = \left(\frac{\Lambda_{\parallel}}{\Lambda_{\perp}} \right)^{2/9} T \quad .$$

The solution of equation (12) is $\tilde{T} = \tilde{T}(x)$

so that

$$\frac{\tilde{T}'}{\tilde{T}} = \left(\frac{\Lambda_{\parallel}}{\Lambda_{\perp}} \right)^{2/9} \frac{d\tilde{T}(x)/dx}{\tilde{T}(x)} \quad . \quad (13)$$

For $\Lambda_{\parallel} \rightarrow 0$ we have $x \rightarrow 0$, and so

$$\frac{d\tilde{T}(x)/dx}{\tilde{T}(x)} \rightarrow \left(\frac{d\tilde{T}(x)/dx}{\tilde{T}(x)} \right)_{x \rightarrow 0} = c_2$$

where c_2 is a constant, and equation (13) becomes

$$\frac{\tilde{T}'}{\tilde{T}} = c_2 \left(\frac{\Lambda_{\parallel}}{\Lambda_{\perp}} \right)^{2/9} \quad . \quad (14)$$

The eigenvalue relationship between Λ_{\perp} and Λ_{\parallel} is now obtained by matching the solutions for \tilde{T}'/\tilde{T} given by equations (11) and (14). This gives the asymptotic dependence of Λ_{\perp} on Λ_{\parallel} for the boundary condition $T'(0) = 0$

$$\Lambda_{\perp} = \frac{c_3}{\Lambda_{\parallel}^{2/7}} \quad .$$

This relationship has also been demonstrated numerically.

The physical reason why the $\tilde{T}'(0) = 0$ boundary condition gives a greater range of instability than $\tilde{T}(0) = 0$ is that it reduces the stabilising perpendicular heat flows at the lower temperature side of the marfe.

Numerical values

Although there is considerable uncertainty concerning both Λ_{\perp} and $R(T)$, it is of interest to investigate numerical values for tokamak conditions. The uncertainty relating to $R(T)$ can be reduced by writing Λ_{\perp} and Λ_{\parallel} in terms of the radiated power fraction \hat{P} defined by

$$\hat{P} = \frac{P_{rad}}{P_{in}} .$$

We also allow variation of the temperature of maximum R by introducing the transformation $R(T) \rightarrow R(\xi T)$. Thus, using the definition of Λ_{\perp} to eliminate nn_i from equation (3) we obtain the radiating layer and the power coming out of the layer.

$$P_{out}^2 = P_{in}^2 \left(1 - \frac{2 S(0)}{\xi \Lambda_{\perp}} \right)$$

and using the power balance relation

$$P_{rad} = P_{in} - P_{out}$$

we obtain the required equation for Λ_{\perp}

$$\Lambda_{\perp} = \frac{S(0)}{\xi \hat{P} \left(1 - \frac{1}{2} \hat{P} \right)} . \quad (15)$$

Then, since

$$\frac{\Lambda_{\parallel}}{\Lambda_{\perp}} = \frac{k_{\parallel}^2 \alpha}{K_{\perp} (dT/dr)_{+}^2}$$

where α is the constant $(K_{\parallel}/T^{5/2})$, we obtain the required equation for Λ_{\parallel}

$$\Lambda_{\parallel} = k_{\parallel}^2 \alpha A^2 S(0) \chi_{\perp} \cdot \frac{n}{P_{in}^2 \hat{P} \left(1 - \frac{1}{2} \hat{P} \right) \xi} \quad (16)$$

where $n\chi_{\perp} = K_{\perp}$ and A is the area, $4\pi^2 a R$, of the plasma surface. Using equations (15) and (16) it is now possible to display the stability diagram of Fig. 1 in terms of the radiation fraction \hat{P} and the variable $n/P_{in}^2 \hat{P} (1 - \frac{1}{2} \hat{P})$.

We consider an example based on the JET plasma, taking $R = 3\text{m}$, $a = 1.4\text{m}$, $k_{\parallel} = 0.1$ corresponding to $q = 3$, $K_{\perp} = 3\text{n} \cdot \text{m}^{-1} \text{s}^{-1}$ and $\alpha = 1.29 \times 10^{22} \text{m}^{-1} \text{s}^{-1} \text{eV}^{-5/2}$, and use the coronal carbon radiation model. Although the applicability of this model is uncertain, it at least displays the qualitative features of the marfe stability boundary. Fig. 4 shows the dependence of the marfe stability boundary on the value of T at which the radiation function peaks, the variation being achieved through ξ . Instability occurs above the curves. It can be seen from the figure that the solution is weakly double-valued at high radiated power fractions. This feature is sensitive to the form of $R(T)$ near $T = 0$. Since the behaviour of $R(T)$ at very low temperatures is not known we have not explored this effect in detail.

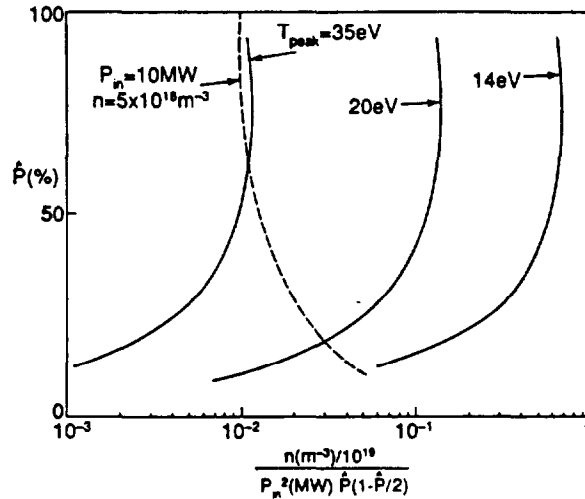


Fig. 4. Marginal marfe stability threshold (for $T'(0) = 0$) for various peak radiation temperatures and a typical operating trajectory ($P_{in} = 10 \text{ MW}$, $n = 5 \times 10^{18} \text{ m}^{-3}$). Marfes are unstable above their respective boundaries.

Given operating conditions, as determined by P_{in} and n , are represented by a line in Fig. 4. For example the line for $P_{in} = 10 \text{ MW}$ and $n = 5 \times 10^{18} \text{ m}^{-3}$ is shown. It is seen that along this line marfes become unstable at reasonable radiation temperatures and that the radiated power fraction to trigger a marfe instability increases with peak radiation temperature. The dominant effect which causes the rapid change in marfe stability with peak radiation temperature is the $T^{5/2}$ dependence of K_{\parallel} . We have also examined the effect of displacing the peak radiation temperature using the transformation $R(T) \rightarrow R(T - T_0)$ and find qualitatively similar results.

Summary

We have presented a generalised approach to the phenomenon of marfe formation. The equilibrium and stability problems are coupled to remove the space variable and to obtain a single equation in which the independent variable is the equilibrium temperature and the dependent variable is the perturbed temperature. The solution of this equation gives a general stability diagram which displays the relationship of marfe stability and the condition for thermal detachment which is approximately the density limit disruption boundary.

References

1. Stringer, T.E., Proceedings of 12th E.P.S. Conference on Controlled Fusion and Plasma Physics, Budapest 1985, 1, 86.
2. Neuhauser, J., Schneider, W. and Wunderlich, R., Nuclear Fusion 26, 1679 (1986).
3. Drake, J.F., Physics of Fluids 30, 2429 (1987).
4. Post, D.E., Jensen, R.V., Tarter, C.B. Grasberger, W.H., and Lokke, W.A., Atomic Data and Nuclear Data Tables 20, 397 (1977).

ANNEX

P.-H. REBUT, A. GIBSON, M. HUGUET, J.M. ADAMS¹, B. ALPER, H. ALTMANN, A. ANDERSEN², P. ANDREW³, M. ANGELONE⁴, S. ALI-ARSHAD, P. BAIGGER, W. BAILEY, B. BALET, P. BARABASCHI, P. BARKER, R. BARNSLEY⁵, M. BARONIAN, D.V. BARTLETT, L. BAYLOR⁶, A.C. BELL, G. BENALI, P. BERTOLDI, E. BERTOLINI, V. BHATNAGAR, A.J. BICKLEY, D. BINDER, H. BINDSLEV², T. BONICELLI, S.J. BOOTH, G. BOSIA, M. BOTMAN, D. BOUCHER, P. BOUCQUEY, P. BREGER, H. BRELEN, H. BRINKSCHULTE, D. BROOKS, A. BROWN, T. BROWN, M. BRUSATI, S. BRYAN, J. BRZOZOWSKI⁷, R. BUCHSE²², T. BUDD, M. BURES, T. BUSINARO, P. BUTCHER, H. BUTTGEREIT, C. CALDWELL-NICHOLS, D.J. CAMPBELL, P. CARD, G. CELENTANO, C.D. CHALLIS, A.V. CHANKIN⁸, A. CHERUBINI, D. CHIRON, J. CHRISTIANSEN, P. CHUILON, R. CLAESEN, S. CLEMENT, E. CLIPSHAM, J.P. COAD, I.H. COFFEY⁹, A. COLTON, M. COMISKEY¹⁰, S. CONROY, M. COOKE, D. COOPER, S. COOPER, J.G. CORDEY, W. CORE, G. CORRIGAN, S. CORTI, A.E. COSTLEY, G. COTTRELL, M. COX¹¹, P. CRIPWELL¹², O. Da COSTA, J. DAVIES, N. DAVIES, H. de BLANK, H. de ESCH, L. de KOCK, E. DEKSNIS, F. DELVART, G.B. DENNE-HINNOV, G. DESCHAMPS, W.J. DICKSON¹³, K.J. DIETZ, S.L. DMITRENKO, M. DMITRIEVA¹⁴, J. DOBBING, A. DOGLIO, N. DOLGETTA, S.E. DORLING, P.G. DOYLE, D.F. DÜCHS, H. DUQUENOY, A. EDWARDS, J. EHRENBERG, A. EKEDAHL, T. ELEVANT⁷, S.K. ERENTS¹¹, L.G. ERIKSSON, H. FAJEMIROKUN¹², H. FALTER, J. FREILING¹⁵, F. FREVILLE, C. FROGER, P. FROISSARD, K. FULLARD, M. GADEBERG, A. GALETSAS, T. GALLAGHER, D. GAMBIER, M. GARRIBBA, P. GAZE, R. GIANNELLA, R.D. GILL, A. GIRARD, A. GONDHALEKAR, D. GOODALL¹¹, C. GORMEZANO, N.A. GOTTARDI, C. GOWERS, B.J. GREEN, B. GRIEVSON, R. HAANGE, A. HAIGH, C.J. HANCOCK, P.J. HARBOUR, T. HARTRAMPF, N.C. HAWKES¹¹, P. HAYNES¹¹, J.L. HEMMERICH, T. HENDER¹¹, J. HOEKZEMA, D. HOLLAND, M. HONE, L. HORTON, J. HOW, M. HUART, I. HUGHES, T.P. HUGHES¹⁰, M. HUGON, Y. HUO¹⁶, K. IDA¹⁷, B. INGRAM, M. IRVING, J. JACQUINOT, H. JAECKEL, J.F. JAEGER, G. JANESCHITZ, Z. JANKOVICZ¹⁸, O.N. JARVIS, F. JENSEN, E.M. JONES, H.D. JONES, L.P.D.F. JONES, S. JONES¹⁹, T.T.C. JONES, J.-F. JUNGER, F. JUNIQUE, A. KAYE, B.E. KEEN, M. KEILHACKER, G.J. KELLY, W. KERNER, A. KHUDOLEEV²¹, R. KONIG, A. KONSTANTELLOS, M. KOVANEN²⁰, G. KRAMER¹⁵, P. KUPSCHUS, R. LÄSSER, J.R. LAST, B. LAUNDY, L. LAURO-TARONI, M. LAVEYRY, K. LAWSON¹¹, M. LENNHOLM, J. LINGERTAT²², R.N. LITUNOVSKI, A. LOARTE, R. LOBEL, P. LOMAS, M. LOUGHLIN, C. LOWRY, J. LUPO, A.C. MAAS¹⁵, J. MACHUZAK¹⁹, B. MACKLIN, G. MADDISON¹¹, C.F. MAGGI²³, G. MAGYAR, W. MANDL²², V. MARCHESE, G. MARCON, F. MARCUS, J. MART, D. MARTIN, E. MARTIN, R. MARTIN-SOLIS²⁴, P. MASSMANN, G. MATTHEWS, H. McBRYAN, G. McCRACKEN¹¹, J. McKIVITT, P. MERIGUET, P. MIELE, A. MILLER, J. MILLS, S.F. MILLS, P. MILLWARD, P. MILVERTON, E. MINARDI⁴, R. MOHANTI²⁵, P.L. MONDINO, D. MONTGOMERY²⁶, A. MONTVAI²⁷, P. MORGAN, H. MORSI, D. MUIR, G. MURPHY, R. MYRNÄS²⁸, F. NAVE²⁹, G. NEWBERT, M. NEWMAN, P. NIELSEN, P. NOLL, W. OBERT, D. O'BRIEN, J. ORCHARD, J. O'ROURKE, R. OSTROM, M. OTTAVIANI, M. PAIN, F. PAOLETTI, S. PAPASTERGIOU, W. PARSONS, D. PASINI, D. PATEL, A. PEACOCK, N. PEACOCK¹¹, R.J.M. PEARCE, D. PEARSON¹², J.F. PENG¹⁶, R. PEPE DE SILVA, G. PERINIC, C. PERRY, M. PETROV²¹, M.A. PICK, J. PLANCOULAIN, J.-P. POFFÉ, R. PÖHLCHEN, F. PORCELLI, L. PORTE¹³, R. PRENTICE, S. PUPPIN, S. PUTVINSKII⁸, G. RADFORD³⁰, T. RAIMONDI, M.C. RAMOS DE ANDRADE, R. REICHLER, J. REID, S. RICHARDS, E. RIGHI, F. RIMINI, D. ROBINSON¹¹, A. ROLFE, R.T. ROSS, L. ROSSI, R. RUSS, P. RUTTER, H.C. SACK, G. SADLER, G. SAIBENE, J.L. SALANAVE, G. SANAZZARO, A. SANTAGIUSTINA, R. SARTORI, C. SBORCHIA, P. SCHILD, M. SCHMID, G. SCHMIDT³¹, B. SCHUNKE, S.M. SCOTT, L. SERIO, A. SIBLEY, R. SIMONINI, A.C.C. SIPS, P. SMEULDERS, R. SMITH, R. STAGG, M. STAMP, P. STANGEBY³, R. STANKIEWICZ³², D.F. START, C.A. STEED, D. STORK, P.E. STOTT, P. STUBBERFIELD, D. SUMMERS, H. SUMMERS¹³, L. SVENSSON, J.A. TAGLE³³, M. TALBOT, A. TANGA, A. TARONI, C. TERELLA, A. TERRINGTON, A. TESINI, P.R. THOMAS, E. THOMPSON, K. THOMSEN, F. TIBONE, A. TISCORNIA, P. TREVALION, B. TUBBING, P. VAN BELLE, H. VAN DER BEKEN, G. VLASES, M. VON HELLERMANN, T. WADE, C. WALKER, R. WALTON³¹, D. WARD, M.L. WATKINS, N. WATKINS, M.J. WATSON, S. WEBER³⁴, J. WESSON, T.J. WIJNANDS, J. WILKS, D. WILSON, T. WINKEL, R. WOLF, D. WONG, C. WOODWARD, Y. WU³⁵, M. WYKES, D. YOUNG, I.D. YOUNG, L. ZANNELLI, A. ZOLFAGHARI¹⁹, W. ZWINGMANN

-
- ¹ Harwell Laboratory, UKAEA, Harwell, Didcot, Oxfordshire, UK.
 - ² Risø National Laboratory, Roskilde, Denmark.
 - ³ Institute for Aerospace Studies, University of Toronto, Downsview, Ontario, Canada.
 - ⁴ ENEA Frascati Energy Research Centre, Frascati, Rome, Italy.
 - ⁵ University of Leicester, Leicester, UK.
 - ⁶ Oak Ridge National Laboratory, Oak Ridge, TN, USA.
 - ⁷ Royal Institute of Technology, Stockholm, Sweden.
 - ⁸ I.V. Kurchatov Institute of Atomic Energy, Moscow, Russian Federation.
 - ⁹ Queens University, Belfast, UK.
 - ¹⁰ University of Essex, Colchester, UK.
 - ¹¹ Culham Laboratory, UKAEA, Abingdon, Oxfordshire, UK.
 - ¹² Imperial College of Science, Technology and Medicine, University of London, London, UK.
 - ¹³ University of Strathclyde, Glasgow, UK.
 - ¹⁴ Keldysh Institute of Applied Mathematics, Moscow, Russian Federation.
 - ¹⁵ FOM-Institute for Plasma Physics "Rijnhuizen", Nieuwegein, Netherlands.
 - ¹⁶ Institute of Plasma Physics, Academia Sinica, Hefei, Anhui Province, China.
 - ¹⁷ National Institute for Fusion Science, Nagoya, Japan.
 - ¹⁸ Soltan Institute for Nuclear Studies, Otwock/Świerk, Poland.
 - ¹⁹ Plasma Fusion Center, Massachusetts Institute of Technology, Boston, MA, USA.
 - ²⁰ Nuclear Engineering Laboratory, Lappeenranta University, Finland.
 - ²¹ A.F. Ioffe Physico-Technical Institute, St. Petersburg, Russian Federation.
 - ²² Max-Planck-Institut für Plasmaphysik, Garching, Germany.
 - ²³ Department of Physics, University of Milan, Milan, Italy.
 - ²⁴ Universidad Complutense de Madrid, Madrid, Spain.
 - ²⁵ North Carolina State University, Raleigh, NC, USA.
 - ²⁶ Dartmouth College, Hanover, NH, USA.
 - ²⁷ Central Research Institute for Physics, Budapest, Hungary.
 - ²⁸ University of Lund, Lund, Sweden.
 - ²⁹ Laboratório Nacional de Engenharia e Tecnologia Industrial, Sacavem, Portugal.
 - ³⁰ Institute of Mathematics, University of Oxford, Oxford, UK.
 - ³¹ Princeton Plasma Physics Laboratory, Princeton University, Princeton, NJ, USA.
 - ³² RCC Cyfronet, Otwock/Świerk, Poland.
 - ³³ Centro de Investigaciones Energéticas, Medioambientales y Tecnológicas, Madrid, Spain.
 - ³⁴ Freie Universität, Berlin, Germany.
 - ³⁵ Institute for Mechanics, Academia Sinica, Beijing, China.